Proceedings of the Canadian Society for Mechanical Engineering International Congress 2022
CSME Congress 2022
June 5-8, 2022, Edmonton, AB, Canada

INFLUENCE OF STRESS-FREE AGING ON MODULUS AND STRENGTH OF 2D KEVLAR® TUBULAR BRAIDED COMPOSITES

Ahmed Samir Ead[1], Xiao Meng[1], Cagri Ayranci[1], Jason P. Carey[1*]
[1]Department of Mechanical Engineering, University of Alberta, Edmonton, Canada
*jpcarey@ualberta.ca

Abstract — Braiding is a manufacturing technique in which material yarns are repeatedly interlaced to create a preform. The preform is impregnated with a polymer matrix to create a braided composite. Several studies have investigated the tensile, compressive and torsional behaviour of braided composites and characterized their mechanical properties. The results of these studies have often displayed large variations between like specimens. One potential explanation of this variation is uncontrolled manufacturing parameters, including the stress-free aging time post cure for these materials. The objective of this study was to experimentally investigate the influence of stress-free aging on the stiffness and strength of tubular braided composites (TBCs). Samples were manufactured from Kevlar-49 (DEN 1420) using a maypole braider at three-braid angles (35º, 45º and 55º). EPON 826 and Lindau LS-81k were used to cure the sample following the manufacturer data sheet. Manufactured TBCs were left to age for three different times (0 weeks, 2 weeks and 6 weeks). Post aging, quasi-static tensile testing of the samples was conducted following ASTM standard D3039 at a loading rate of 1 mm/min. To measure strain, Digital Image Correlation (DIC) was used. Images were taken every 2 seconds for the duration of the tensile test and processed in imaging software DaVis®. Results from the study were mixed for the different braid angles. For 35º and 45º, there was no statistically significant change in the longitudinal modulus, yield strength and failure strain for the different aged samples. For the 55º samples, there was an 8.43% increase in Young's Modulus and a 15.04% increase in ultimate tensile strength. Due to the architecture of the braids, at higher braid angles, the transverse properties of the resin are more pronounced. The increased strength and stiffness of the resin post aging results in an overall increase in the strength and stiffness of the higher angle composites, confirming the changes in properties of thermosets documented in literature. Further investigation over a larger braid angle range and for longer post-cure times are crucial to confirm findings.

Keywords-braided composites, advanced manufacturing, resin aging, tubuluar braided composites

I. INTRODUCTION

Composites consist of two or more constituents joined together to produce a non-homogenous material with tailorable properties. Braiding is a composite manufacturing technique in which yarns of one or more materials are interlaced over the length of a mandrel to create a preform. This preform is impregnated with a matrix, typically a polymer, to create the braided composite. When a cylindrical mandrel is used, the resulting hollow braided composite is called a tubular braided composite (TBC). Figure 1 shows a typical TBC. Due to their high strength-to-weight and stiffness-to-weight ratios, TBCs have a wide range of potential applications including construction, sports and medicine [1].

Braided preforms are typically manufactured using a rotary braider in which carriers with bobbins of the fibrous material move in predefined serpentine paths. During this motion, yarns are deposited on a translating mandrel to create the braided preform. Figure 2 shows a schematic of the preform braiding process. Matrix impregnation is either a manual or va-

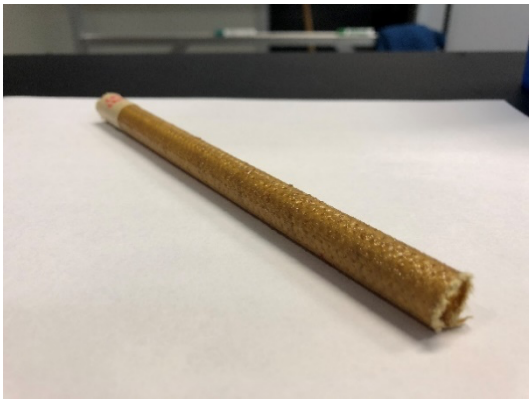

Figure 1. A tubular braided composite

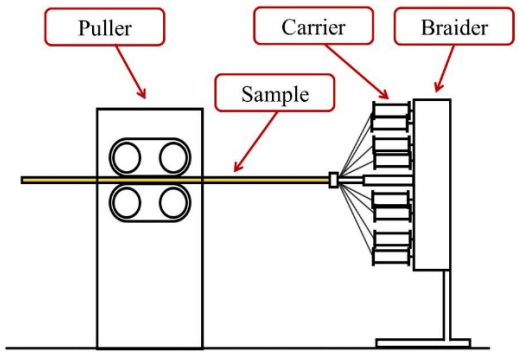

Figure 2. Schematic of braid manufacture line. Yarns from carriers are deposited on the mandrel pulled forward at a predetermined speed.

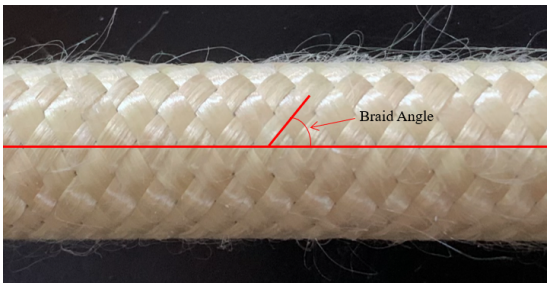

Figure 3. Preform showing the braid angle as the angle between the interlacing yarns and the longitudinal axis of the braid

-cuum assisted process [2]. Several manufacturing parameters influence the final properties of TBCs, however, braid angle is the most significant in determining the final stiffness, strength and rigidity of the composites. Braid angle is defined as the angle between the yarns and the longitudinal axis of the braid. Figure 3 shows the braid angle labelled on a preform.

II. Literature Review

The mechanical properties of TBC are well documented in the literature. Several studies have looked into the kinematics of the braiding process. These studies have focused on developing equations that relate braider rotational speed and puller translational speed to the final braid angle [3]–[7]. A wealth of literature exists on the characterization of TBCs and studying their mechanical properties [8]–[13].

Studies with TBCs have shown high variation between the documented properties of composites manufactured with the same parameters. These variations can often exceed 10% between samples. Sample manufacturing is a primarily manual process and sample repeatability is difficult to attain. One potential aspect of sample repeatability is the stress-free aging of the manufactured composite samples post cure. This is defined as the elapsed time from cure to testing for the composites. The effect of aging on the mechanical properties of thermoset polymers and some polymer composites has been documented in a few studies. Si et al. investigated the influence of thermal-oxidative aging on the mechanical properties of epoxy asphalt. Results showed that the tensile strength of the epoxy asphalt increased due to post-cure aging [14]. Kong et al. showed that the elastic modulus of network epoxy resin increased with post-curing time over the course of seven days. Results were explained to be a consequence of an excess of trapped free volume in the thermoset polymer after curing. As the thermoset resin approaches thermodynamic equilibrium post cure, free volume is lost. This limits the molecular mobility within the resin, increasing elastic modulus [15]. Although a wealth of literature is available on the effect of hygrothermal aging on composite behaviour, very few have looked into stress-free aging. Chiao et al. found that Kevlar® and epoxy composites displayed no change in strength after stress-free aging for five and ten years [16]. Odegard and Bandyopadhyay concluded that the studies investigating the influence of aging on the mechanical properties contradicted each other. Their review indicates that several studies disagreed as to the positive or negative impact of stress-free aging on the elastic modulus and strength of epoxy resins and epoxy composites [17].

While it is clear that some studies have investigated the influence of aging on epoxy and epoxy composites, results have been inconclusive. Further, no studies have investigated the influence of the stress-free aging on braided composites. With the repeatability issue that arises during manufacturing, the post-cure aging phenomenon found in previous studies provides a plausible explanation to the high variation seen in the experimental data collected from TBCs. Accordingly, the objective of this study is to experimentally investigate the influence of stress-free aging on the mechanical properties of TBCs.

III. Methodology

A. Materials

To manufacture TBCs for this work, 1420 Den Kevlar® 49 (DuPont, Wilmington, Delaware, USA), Epon 826 (Hexion Inc., Ohio, USA) epoxy resin with Lindau LS-81K (Lindau Chemicals Inc., South Carolina, USA) hardener were used. Table I shows the mechanical properties of the materials used.

TABLE I. MATERIAL USED IN STUDY AND MECHANICAL PROPERTIES AS FOUND IN [1] AND [18]

Material	Tensile Strength (GPa)	Tensile Modulus (GPa)	Failure Strain (%)
Kevlar 49	3.6	112-138	2.4
Epon 826 (with LS-81K)	0.074	2.7	5

B. *Sample Manufacturing*

Samples were manufactured following the methodology highlighted in previous work by Ead et al. [9]. Braided preforms were manufactured using a rotary maypole braider (Steeger HS140/36-91, Steeger GmbH and Co., Wuppertal, West Germany) and a puller mechanism. Yarns of Kevlar® were spooled onto 36 carriers. Carriers were loaded onto the rotary braider. Yarns were interlaced onto a 7/16'' aluminium mandrel at three different braid angles (35°, 45° and 55°). A LabVIEW™ software was used to control braider rotational speed and puller translational speeds. Preforms for this study were manufactured in a diamond one-over-one-under pattern. Figure 4 shows an image of a sample preform manufactured at 35° and a schematic of the unit cell of the manufactured TBC preforms.

Braided preforms were carefully transferred onto Teflon mandrels and manually impregnated with a 1:1 weight mixture of Epon 826 epoxy resin and Lindau LS-81K hardener. Following the resin manufacturer data sheet, samples were cured in a square oven at 66°C for 90 mins, 85°C for 60 minutes and 150°C for 180 minutes [18]. Once the cure cycles were completed, composite TBC samples were removed from the Teflon mandrels and cut to a sample length of 7 inches. The cross-sectional area of the TBCs was measured using a digital Vernier caliper (Mastercraft Digital Caliper 6-inch, Mastercraft tools, Kirkwood, MO) and recorded. For each sample, cross-sectional

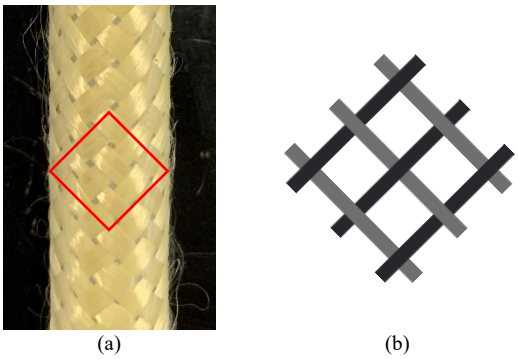

(a) (b)

Figure 4. Image of a (a) 45° preform highlighting the one-over-one under pattern and a (b) unit cell schematic for a regular braid preform.

Figure 5. Cured TBC samples manufactured at three braid angles, 35, 45 and 55 degrees.

area was measured and calculated at three points along the length of the TBC sample. Cross sectional area measurements were then averaged. Figure 5 shows three manufactured TBC samples, one at each of the tested braid angles used in this study.

For post-cure aging, TBC samples were stored in airtight containers at standard ambient temperature and pressure. Three aging periods were chosen for this work: 0 weeks, 2 weeks and 6 weeks based on previous research [15]. Three samples were tested per braid angle and aging interval for a total of 27 samples. Table II shows the experimental matrix of this study.

TABLE II. TBC SAMPLE EXPERIMENTAL MATRIX

Angle	Aging Time (weeks)	Number of Samples
35°	0	3
	2	3
	6	3
45°	0	3
	2	3
	6	3
55°	0	3
	2	3
	6	3

C. *Sample Testing*

Prior to testing, each sample was attached to steel end tabs using two-part epoxy (Henkel AG & Company, KHaA, Düsseldort, Germany). With end tabs attached, TBC samples were tied to aluminium rails with hose clamps for 24 hours to allow the two-part epoxy time to cure while maintaining braid alignment. To prepare samples for strain measurement, tabbed TBC samples were painted in black matte paint (Painter's Touch Flat Black, Rust-Oleum Corp, Concord, ON, Canada). Once painted and dried, a white speckle pattern (4230 Transparent White, Auto Air-Colors, East Granby, CT) was applied to the sample using an airbrush (Paasche H Series, Paasche Air Brush Co., Chicago, IL). The whi-

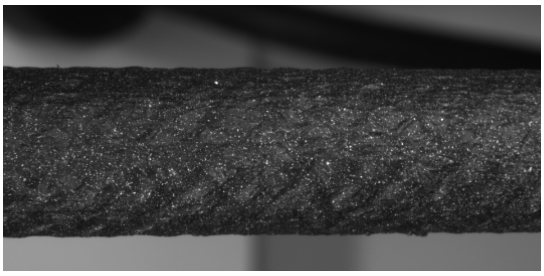

Figure 6. Zoomed in image of a 45° speckled TBC sample.

-te speckles against the black TBC samples provided enough contrast for strain data collection. A sample TBC prepared for testing is shown in Figure 6.

Quasi-static tensile testing of TBC samples was performed using a hydraulic MTS machine (MTS Systems, Eden Prairie, MN) following ASTM standard D3039 [19]. Samples were pinned to the MTS grips using metal dowels. To apply the tensile loads to the samples, a 1000 lb load cell was used. For this study, samples were loaded at a strain rate of 1 mm/min as this resulted in sample failure within 1 to 10 minutes of test initiation as specified by ASTM standards. A data acquisition program collected the load data from the MTS machine every 0.01 seconds. To collect the strain data, an imaging technique similar to that highlighted in Lepp and Carey was followed [20]. Two scientific cameras (Basler acA3800-10gm, Basler AG, Ahrensburg, Germany) were positioned at an approximately 22° offset from the horizontal. The cameras acquired images of the samples every two seconds throughout the duration of the tensile test. A MATLAB® code was written to control image acquisition and file storage for each sample tested. Tensile load was increased until yielding was observed in the load response of the sample or pseudo-necking occurred. Figure 7 shows the experimental setup for the quasi-static tensile tests conducted in this study.

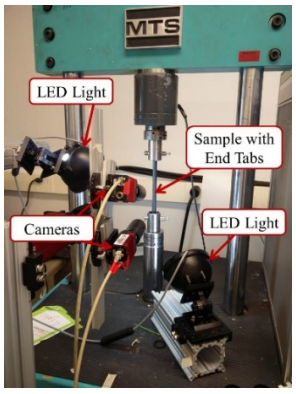

Figure 7. Experimental setup used for quasi-static tensile testing of aged TBC samples

D. DIC Image Analysis

Images collected during the tensile tests were processed using 3D digital image correlation in image processing software DaVis® (LaVision, Göttingen, Germany). DIC is a contact-free strain measurement technique that traces the motion of speckles between images throughout the tensile test and uses a correlation algorithm to calculate deformation vectors between successive images. These deformation vectors can then used to produce a strain map along the braid in the three principal directions. The validity and precision of using 3D DIC to analyse strain across a tubular braided composite has been justified by Melenka et al. [21]. Once a strain map is produced, DaVis® allows users to calculate the average global strain over a length of the sample with a virtual extensometer function. Prior to producing deformation and strain results, an intensity normalization filter and sliding average Gaussian filter were applied to each pair of images. These improve the ability of the software to accurately calculate the displacements of the speckles on the braid surface. Once displacements were calculated for each pair of images, a virtual extensometer was used to calculate the average global longitudinal strain from each pair of images. Figure 8 shows the strain map on a sample with the virtual extensometer highlighted.

IV. Results

Load data collected and converted from the load cell was converted to stress data by dividing by the cross-sectional areas measured post-sample manufacture. Stress data was plotted against the corresponding strain data produced from DaVis for each of the 27 tested samples. For each three samples tested at a particular braid angle and aging time, the stress-strain plots were averaged. Figure 9 shows the

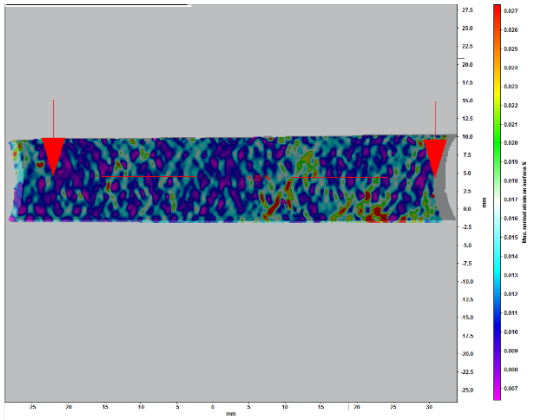

Figure 8. Maximum surface strain on 55° braid immediately before failure. Virtual extensometer length is indicated by the red line between the two arrows.

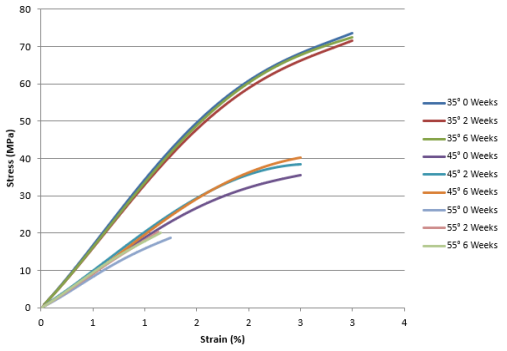

Figure 9. Plots of the average stress-strain behavior of each experimental condition tested.

average stress-strain results for each of the testing conditions.

To calculate the longitudinal elastic modulus of the tested samples, ASTM standard E111-17 for measuring young modulus was followed. Equation (1) shows the statistical formula used to calculate the longitudinal elastic modulus from the collected stress and strain data [22]. Yield strength was measured using the 0.2% strain offset method. Table III shows the results of elastic modulus and yield strength from the data collected.

$$E_x = \frac{\sum_i^K (\sigma_i \varepsilon_i) - K\bar{\sigma}\bar{\varepsilon}}{\sum_i^K \sigma_i^2 - K\bar{\sigma}^2} \quad (1)$$

where E_x is longitudinal elastic modulus, σ_i and ε_i are the stress and strain values of a data point, K is the total number of data points and $\bar{\sigma}$ and $\bar{\varepsilon}$ are the average stress and strain for all data points.

TABLE III. AVERAGE MODULUS AND STRENGTH VALUES CALCULATED FROM THE DIFFERENT TESTED TBC SAMPLES

Braid Angle (°)	Aging Time (weeks)	Average Elastic Modulus (GPa)	Average Yield Strength (MPa)
35	0	3.45±0.15	59.9±0.32
	2	3.34±0.13	57.7±2.08
	6	3.39±0.02	59.8±1.02
45	0	2.03±0.05	32.5±2.49
	2	2.05±0.05	34.7±2.39
	6	2.13±0.02	35.7±1.87
55	0	1.78±0.05	18.65*
	2	1.92±0.09	22.08*
	6	1.94±0.07	20.83*

* values for yield data could not be collected due to sample failure, fracture strength is reported for these samples.

V. Discussion

Stress-strain plots in Figure 9 as well as the average experimental results in Table III show typical properties of TBCs. TBCs manufactured at lower braid angles have higher longitudinal modulus and strength. At these lower angles, orientation of the yarns is closer to the longitudinal direction of the braid results in higher stiffness imparted by the reinforcement phase. The opposite is seen at higher braid angles. These results agree with the available literature on the tensile properties of TBCs.

For the influence of aging time on the mechanical properties of tubular braided composites, initial results from this study seem to indicate that stress-free aging does not have a significant impact on the stiffness and strength of TBCs. Percentage changes in the average elastic modulus ranged from -3.30% for the 35° TBC samples between 0 and 2 weeks to 7.65% for the 55° TBC samples between 0 and 2 weeks. Data collected for this study shows that percentage changes become larger and more positive as braid angle increases. One possible explanation for this phenomenon is related to braid architecture. At higher braid angles, the resin contributes more significantly to the overall longitudinal behavior of the TBC. The influence of stress-free aging on the resin found by Kong et al. would explain the increased stiffness and strength of resin and the increase in TBC stiffness and strength at higher braid angles. Similar results were found for the yield strength data [15].

VI. Conclusion

The purpose of this study was to investigate the influence of post-cure stress-free aging on the properties of TBCs. Although some literature has investigated the influence of aging on epoxy and epoxy composites, results from these studies have showed mixed results with regards to the changes in the properties of composites as related to post-cure aging time. Stress-free aging was hypothesized to be a potential reason behind the large variation seen in the tensile data collected from TBC. No literature is available on the impact of stress-free aging on the behaviour of TBCs.

TBC samples were manufactured at three different braid angles (35°, 45° and 55°) and tested in tension after 0,2 and 6 weeks of curing. Three TBC samples were tested for each configuration. DIC was used to collect strain data for this study. Initial results from this work seem to indicate that post-cure aging time does not have a significant on lower braid angles, however, might have a higher impact on the behaviour of higher angle TBCs. More experimental studies involving more braid angles and large post-cure aging times are critical to confirm the preliminary results of this work.

References

[1] J. P. Carey, "Introduction to braided composites," *Handbook of Advances in Braided Composite Materials: Theory, Production,*

Testing and Applications, pp. 1–21, Jan. 2017, doi: 10.1016/B978-0-08-100369-5.00001-5.
[2] G. W. Melenka *et al.*, "Manufacturing processes for braided composite materials," *Handbook of Advances in Braided Composite Materials: Theory, Production, Testing and Applications*, pp. 47–153, Jan. 2017, doi: 10.1016/B978-0-08-100369-5.00003-9.
[3] J. H. van Ravenhorst and R. Akkerman, "Circular braiding take-up speed generation using inverse kinematics," *Composites Part A: Applied Science and Manufacturing*, vol. 64, pp. 147–158, 2014, doi: 10.1016/j.compositesa.2014.04.020.
[4] G. W. Du and P. Popper, "Analysis of a circular braiding process for complex shapes," *Journal of the Textile Institute*, vol. 85, no. 3, pp. 316–337, 1994, doi: 10.1080/00405009408631277.
[5] Q. Zhang, D. Beale, and R. M. Broughton, "Analysis of circular braiding process, part 1: Theoretical investigation of kinematics of the circular braiding process," *Journal of Manufacturing Science and Engineering, Transactions of the ASME*, vol. 121, no. 3, pp. 345–350, 1999, doi: 10.1115/1.2832687.
[6] Q. Zhang, D. Beale, R. M. Broughton, and S. Adanur, "Analysis of circular braiding process, part 2: Mechanics analysis of the circular braiding process and experiment," *Journal of Manufacturing Science and Engineering, Transactions of the ASME*, vol. 121, no. 3, pp. 351–359, 1999, doi: 10.1115/1.2832688.
[7] D. Brunnschweiler, "Braids and braiding," *Journal of the Textile Institute*, vol. 44, pp. 666–686, 1953.
[8] C. Ayranci and J. P. Carey, "Effect of diameter in predicting the elastic properties of 2D braided tubular composites," *Journal of Composite Materials*, vol. 44, no. 16, pp. 2031–2044, 2010, doi: 10.1177/0021998310369599.
[9] A. S. Ead, C. Ayranci, and J. P. Carey, "An Experimental Study of the Creep Behavior of Braided Composites," 2019. doi: 10.33599/nasampe/s.19.1408.
[10] B. Bruni-bossio, C. Ayranci, J. P. Carey, T. Omonov, and J. Curtis, "Experimental testing of the tensile elastic properties of cellulose braided composites," *Composites Part B*, vol. 166, no. October 2018, pp. 542–548, 2019, doi: 10.1016/j.compositesb.2019.02.052.
[11] B. M. Bruni-bossio, G. W. Melenka, C. Ayranci, and J. P. Carey, "Micro-computed tomography analysis of natural fiber and bio-matrix tubular-braided composites," 2019, doi: 10.1177/0021998319853023.
[12] C. Ayranci and J. Carey, "2D braided composites: A review for stiffness critical applications," *Composite Structures*, vol. 85, no. 1, pp. 43–58, 2008, doi: 10.1016/j.compstruct.2007.10.004.
[13] C. Ayranci and J. P. Carey, "Predicting the longitudinal elastic modulus of braided tubular composites using a curved unit-cell geometry," *Composites Part B: Engineering*, vol. 41, no. 3, pp. 229–235, 2010, doi: 10.1016/j.compositesb.2009.10.006.
[14] J. Si *et al.*, "Influence of thermal-oxidative aging on the mechanical performance and structure of cold-mixed epoxy asphalt," *Journal of Cleaner Production*, vol. 337, Feb. 2022, doi: 10.1016/J.JCLEPRO.2022.130482.
[15] E. S. Kong, G. L. Wilkes, J. E. McGrath, A. K. Banthia, Y. Mohajer, and M. R. Tant, "Physical aging of linear and network epoxy resins," *Polymer Engineering & Science*, vol. 21, no. 14, pp. 943–950, 1981, doi: 10.1002/pen.760211413.
[16] T. T. Chiao, R. L. Moore, and T. H, "No-Stress Aging of Aramid / Epoxy Composites," pp. 98–100, 2019.
[17] G. M. Odegard and A. Bandyopadhyay, "Physical aging of epoxy polymers and their composites," *Journal of Polymer Science, Part B: Polymer Physics*, vol. 49, no. 24, pp. 1695–1716, 2011, doi: 10.1002/polb.22384.
[18] Hexion, "Technical Data Sheet for Epoxy Resin System 826 862 LS-81K," 2022. Accessed: Feb. 09, 2022. [Online]. Available: https://www.hexion.com/en-US/product/sf-8017-epoxy-resin-system-826-862-ls-81k
[19] ASTM INTERNATIONAL, "D3039/D3039M-08: Standard Test Method for Tensile Properties of Polymer Matrix Composite Materials," 2014. Accessed: Feb. 09, 2022. [Online]. Available: https://compass.astm.org/document/?contentCode=ASTM%7CD3039_D3039M-08%7Cen-US&proxycl=https%3A%2F%2Fsecure.astm.org&fromLogin=true
[20] E. A. Lepp and J. P. Carey, "An examination of initial structural degradation in tubular braided composites through region-by-region strain analysis:," *https://doi.org/10.1177/1558925020978325*, vol. 15, Dec. 2020, doi: 10.1177/1558925020978325.
[21] G. W. Melenka and J. P. Carey, "Experimental analysis of diamond and regular tubular braided composites using three-dimensional digital image correlation:," *https://doi.org/10.1177/0021998317695418*, vol. 51, no. 28, pp. 3887–3907, Feb. 2017, doi: 10.1177/0021998317695418.
[22] ASTM INTERNATIONAL, "E111-17: Standard Test Method for Young's Modulus, Tangent Modulus , and Chord Modulus," 2010. doi: 10.1520/E0111-04R10.